

EVOLUTION OF UNCONDITIONAL DISPERSAL IN PERIODIC ENVIRONMENTS

SEBASTIAN J. SCHREIBER AND CHI-KWONG LI

ABSTRACT. Organisms modulate their fitness in heterogeneous environments by dispersing. Prior work shows that there is selection against “unconditional” dispersal in spatially heterogeneous environments. “Unconditional” means individuals disperse at a rate independent of their location. We prove that if within-patch fitness varies spatially and between two values temporally, then there is selection for unconditional dispersal: any evolutionarily stable strategy (ESS) or evolutionarily stable coalition (ESC) includes a dispersive phenotype. Moreover, at this ESS or ESC, there is at least one sink patch (i.e. geometric mean of fitness less than one) and no sources patches (i.e. geometric mean of fitness greater than one). These results coupled with simulations suggest that spatial-temporal heterogeneity due to abiotic forcing result in either an ESS with a dispersive phenotype or an ESC with sedentary and dispersive phenotypes. In contrast, spatial-temporal heterogeneity due to biotic interactions can select for higher dispersal rates that ultimately spatially synchronize population dynamics.

1. INTRODUCTION

1 Plants and animals often live in landscapes where environmental conditions vary in space
2 and time. These environmental conditions may include abiotic factors such as light, space,
3 and nutrient availability or biotic factors such as prey, competitors, and predators. Since
4 the fecundity and survivorship of an individual depends on these factors, an organism may
5 decrease or increase its fitness by dispersing across the environment. Understanding how
6 natural selection acts on dispersal in heterogeneous environments has been the focus of
7 much theoretical and empirical work [1–21].

8 In spatially heterogeneous environments, the general consensus is that there is selection
9 against unconditional dispersal [3, 8, 12, 16, 20]. Here, unconditional refers to the assumption
10 that individuals disperse at a rate independent of their location. Using reaction-diffusion
11 equations, Dockery et al. [12] proved that for two competing populations only differing

12 in their diffusion constant, the population with the larger diffusion constant is excluded.
 13 In [16, 20], similar results were proven for populations with non-overlapping generations
 14 living in a patchy environment. Alternatively, in temporally but not spatially heterogenous
 15 environments, Hutson et al. [15] proved that dispersal rates are a selectively neutral trait
 16 for reaction-diffusion models and, thereby, confirmed the numerical observations of McPeck
 17 and Holt [8] for discrete-time, two-patch models. These results imply that the slightest cost
 18 of dispersal would result in selection against dispersal in purely temporally heterogenous
 19 environments.

20 When there is a mixture of spatial and temporal heterogeneity, the interaction between
 21 competing dispersal phenotypes becomes more subtle. Numerically simulating discrete-time,
 22 two-patch models, McPeck and Holt [8], Parvinen [20], and Mathias et al. [13] found that
 23 more dispersive phenotypes could displace more sedentary phenotypes for certain forms
 24 of spatial-temporal heterogeneity, while evolutionarily stable coalitions of sedentary and
 25 dispersal phenotypes are possible for other forms of spatial-temporal heterogeneity. Hutson et
 26 al. [15] proved that similar phenomena could occur for reaction diffusion equations. However,
 27 analytical criteria distinguishing these outcomes remain elusive.

28 In this article, we consider the evolution of dispersal for a general class of multi-patch
 29 difference equations varying periodically in time. This periodic variation can be either due
 30 to biotic interactions or abiotic forcing. Our main goals are to analytically identify potential
 31 evolutionarily stable strategies or coalitions for dispersal, characterize the spatial-temporal
 32 patterns of fitness generated by populations playing these dispersal strategies, and use our
 33 results to compare evolutionary outcomes for oscillations due to abiotic forcing versus oscil-
 34 lations due to biotic interactions.

35

2. MODELS AND ASSUMPTIONS

36 To understand the formation of evolutionarily stable coalitions of dispersive phenotypes,
 37 we consider a population consisting of m phenotypes dispersing in an environment consist-
 38 ing of n patches. Let $x_i^j(t)$ denote the abundance of phenotype i in patch j . The fitness
 39 of an individual in patch j is assumed to be of the form $f^j(t, \sum_{i=1}^m x_i^j(t))$. In particular,
 40 this assumption implies that phenotypes only differ demographically in their propensity to
 41 disperse. Moreover, we assume that $f^j(t, \cdot)$ is of period p . This periodicity may arise from
 42 exogenous forcing or biological interactions (e.g. over compensating density dependence or
 43 predator-prey interactions). While we do not explicitly model interactions with other species,

44 our formulation is sufficiently general to be viewed as the dynamics of a particular species
 45 embedded within a web of interacting species.

46 We assume that the fraction of phenotype i dispersing from any given patch is d_i . Of
 47 the individuals dispersing from patch j , a fraction S_{kj} go to patch k . We call $S = (S_{kj})$
 48 the dispersal matrix and it characterizes how dispersing individuals are redistributed across
 49 the landscape. Under these assumptions, the interacting phenotypes exhibit the following
 50 population dynamics:

$$x_i^j(t+1) = (1 - d_i) f^j \left(t, \sum_{l=1}^m x_l^j(t) \right) x_i^j(t) + d_i \sum_{k=1}^n S_{jk} f^k \left(t, \sum_{l=1}^m x_l^k(t) \right) x_i^k(t)$$

51 To express this model more succinctly, let $\mathbf{x}^j = (x_1^j, \dots, x_m^j)$ be the vector of abundances
 52 of the m phenotypes in patch j , $\mathbf{x}_i = (x_i^1, \dots, x_i^n)^T$ (where T denotes transpose) be the
 53 vector of abundances of strategy i across the n patches, and $\|\mathbf{x}^j\| = \sum_{i=1}^m x_i^j$ denote the
 54 total abundance of individuals in patch j . Let \mathbf{x} be the matrix with entries x_i^j , $\mathbf{F}(t, \mathbf{x})$ be
 55 a diagonal matrix whose j -th diagonal element is $f^j(t, \|\mathbf{x}^j\|)$, and $\mathbf{S}(d_i) = (1 - d_i)I + d_i S$
 56 where I is the identity matrix. With this notation, the model is represented more succinctly
 57 as

$$(2.1) \quad \mathbf{x}_i(t+1) = \mathbf{S}(d_i) \mathbf{F}(t, \mathbf{x}(t)) \mathbf{x}_i(t) \quad i = 1, \dots, m.$$

58 About this model, we make three assumptions throughout this manuscript.

59 **A1:** The dispersal matrix \mathbf{S} is irreducible and column stochastic (i.e. S has nonnegative
 60 entries, and the entries of each column sum up to one).

61 **A2:** (2.1) has a positive period- p point $\hat{\mathbf{x}}(1), \dots, \hat{\mathbf{x}}(p)$ i.e. $\|\hat{\mathbf{x}}_i(t)\| > 0$ and $\|\hat{\mathbf{x}}^j(t)\| > 0$
 62 for all i, j, t , and

$$(2.2) \quad \prod_{t=1}^p \mathbf{S}(d_i) \mathbf{F}(t, \hat{\mathbf{x}}(t)) \hat{\mathbf{x}}_i(1) = \hat{\mathbf{x}}_i(1) \text{ for all } i.$$

63 **A3:** $\mathbf{F}(t, \mathbf{x})$ is continuous in \mathbf{x} .

64 Assumption **A1** ensures that individuals or their decedents can move from any patch to any
 65 other patch after sufficiently many generations and there is no direct cost to dispersal. As-
 66 sumption **A2** implies that the phenotypes are coexisting in a periodic fashion and occupying
 67 all the patches. Assumption **A3** is a basic regularity assumption met by most models.

68

3. MAIN RESULTS

69 We are primarily interested in understanding when a periodically fluctuating collection of
 70 phenotypes can not be invaded by any other phenotype, and what are the spatial-temporal
 71 patterns of fitness at these potential evolutionary end states. To state our main results
 72 precisely, we need two sets of definitions.

73 **Invasion rates, Nash equilibria and evolutionary stability.** Let $\mathbf{d} = (d_1, \dots, d_m)$ the
 74 coalition of strategies played by the resident population. If we added a “mutant” phenotype
 75 with dispersal rate \tilde{d} into the population and this mutant population $\mathbf{y} = (y^1, \dots, y^n)$ is very
 76 small, then the resident’s population dynamics are initially barely influenced by the mutant’s
 77 population dynamics and the mutant’s dynamics are approximately given by a linear model

$$\mathbf{y}(t+1) = \mathbf{S}(\tilde{d})\mathbf{F}(t, \mathbf{x}(t))\mathbf{y}(t).$$

78 By standard linearization theorems (see, e.g., [22]), this approximation is valid when the size
 79 of the mutant population is small and the periodic point in **A2** is hyperbolic.

80 The initial fate of the mutant population depends on the *invasion rate of strategy \tilde{d} against*
 81 *the resident population playing strategies \mathbf{d} :*

$$\mathcal{I}(\mathbf{d}; \tilde{d}) = \varrho \left(\prod_{t=1}^p \mathbf{S}(\tilde{d})\mathbf{F}(t, \hat{\mathbf{x}}(t)) \right)^{1/p}$$

82 where $\mathbf{x}(t)$ has period p and $\varrho(\mathbf{A})$ corresponds to the largest eigenvalue for a non-negative
 83 matrix \mathbf{A} . If the invasion rate $\mathcal{I}(\mathbf{d}; \tilde{d})$ is greater than one, then the mutant population
 84 grows when its size is small. The ultimate fate of the mutant and resident after the mutant
 85 increases depends on the details of full non-linear model of the resident and invader dynamics.
 86 In particular, following an invasion the asymptotic dynamics in general may no longer be
 87 periodic (i.e. satisfy **A2**). There are many cases where post-invasion dynamics will remain
 88 periodic (e.g. periodically forced competitive systems as discussed in section 4.1 or when
 89 there is attractor inheritance for a sufficiently small mutation [23]).

90 If the invasion rate $\mathcal{I}(\mathbf{d}; \tilde{d})$ is less than one, then the mutant population declines exponen-
 91 tially when rare and it can not invade. Finally, if $\mathcal{I}(\mathbf{d}; \tilde{d}) = 1$, then a mutant may increase
 92 or decrease when rare depending on the details of the nonlinearities of the full model. How-
 93 ever, if it increases, then it does so at a subexponential rate and, therefore, may be highly
 94 vulnerable to stochastic extinction. An important consequence of our assumption **A2** is that

95 the invasion rate of mutants with the same strategy as a resident equals one i.e. $\mathcal{I}(\mathbf{d}; \tilde{d}) = 1$
 96 whenever $\tilde{d} = d_i$ for some i .

97 Using the invasion rates of mutant strategies, we can define several concepts associated
 98 with evolutionary stability. A coalition of strategies \mathbf{d} with $m > 1$ is a *mixed Nash equilibrium*
 99 provided that

$$(3.3) \quad \mathcal{I}(\mathbf{d}; \tilde{d}) \leq 1 \text{ for all } \tilde{d} \in [0, 1]$$

100 In other words, a mixed Nash equilibrium is a set of strategies in which all mutant strategies
 101 are unlikely to invade due to vulnerability to stochastic extinction. When $m = 1$, a strategy
 102 satisfying (3.3) is called simply a *Nash equilibrium*. Under the stronger assumption that rare
 103 mutants decline exponentially to extinction (i.e. $\mathcal{I}(\mathbf{d}; \tilde{d}) < 1$ for all $\tilde{d} \notin \{d_1, \dots, d_m\}$), \mathbf{d} is
 104 an *evolutionarily stable coalition (ESC)* if $m > 1$ or an *evolutionarily stable strategy (ESS)*
 105 if $m = 1$ [24]. More generally, every ESS (respectively, ESC) is a (mixed) Nash equilibrium.

106 **Sources, sinks, and balanced patches.** Pulliam [6] introduced the notion of sources and
 107 sink patches for a population at equilibrium. In source patches birth rates exceed death rates,
 108 while in sink patches death rates exceed birth rates. Here, we extend Pulliam’s definition to
 109 population exhibiting periodic fluctuations in abundance. A patch is a source if births exceed
 110 deaths “on average” across years, while a patch is a sink if deaths exceed births “on average”
 111 across years. For fitnesses varying in time, the appropriate “average” is the geometric mean:

$$\bar{f}_j = \left(\prod_{t=1}^p f^j(t, \|\hat{\mathbf{x}}^j(t)\|) \right)^{1/p}.$$

112 If $\bar{f}_j < 1$, then patch j is a *sink*. If $\bar{f}_j > 1$, then patch j is a *source*. Following McPeck and
 113 Holt [8], we say patch j is *balanced* if $\bar{f}_j = 1$. Individuals remaining in a balanced patch, on
 114 average exactly replace themselves.

115 **Main Results.** We have two main results. Our first result implies that if there is spatial
 116 heterogeneity in the within-patch fitnesses under equilibrium conditions, then no coalition of
 117 distinctive phenotypes can coexist, there is selection for slower dispersers, and the landscape
 118 supports source and sink patches. In particular, this result implies that for populations
 119 at equilibrium and playing a Nash equilibrium, all patches must be balanced. This result
 120 follows from [16] and generalizes earlier work of Hasings [3] and Parvinen [20] by allowing
 121 for non-diffusive patterns of dispersal (i.e. S need not be symmetric).

122 **Proposition 1.** *If $p = 1$ and $\mathbf{F}(1, \hat{\mathbf{x}}(1))$ is not scalar (i.e. there is spatial heterogeneity),*
 123 *then all the d_i are equal and positive, $\mathcal{I}(\mathbf{d}; \tilde{d}) > 1$ for all $0 \leq \tilde{d} < d_1$, and at least one patch*
 124 *is a sink and at least one patch is a source.*

125 *Proof.* Let \mathbf{A} be the diagonal matrix $\mathbf{F}(1, \hat{\mathbf{x}}(1))$ with diagonal entries $A_{jj} = f^j(1, \|\hat{\mathbf{x}}^j(1)\|)$.
 126 Since \mathbf{A} is not scalar, Theorem 3.1 in [16] implies that $\varrho(\mathbf{S}(d)\mathbf{A})$ is a strictly decreasing
 127 function of $d \in [0, 1]$. Assumption **A2** implies that $\varrho(\mathbf{S}(d_i)\mathbf{A}) = 1$ for all i . Hence, all of the
 128 d_i are equal and $\mathcal{I}(\mathbf{d}; \tilde{d}) > 1$ for all $0 \leq \tilde{d} < d_1$. The d_i can not equal zero as this would imply
 129 that $\mathbf{F}(1, \hat{\mathbf{x}}_i(1))$ is the identity matrix contradicting the assumption that it is non-scalar.
 130 Since $\mathbf{S}(d_1)$ is column stochastic and \mathbf{A} is non-scalar, $\max_i A_{ii} > \varrho(\mathbf{S}(d_1)\mathbf{A}) = 1 > \min_i A_{ii}$.
 131 Hence, there is a source patch and a sink patch.

132 ■

133 Our second result concerns period 2 environments. In contrast to populations at equilib-
 134 rium, this result implies that any ESS or ESC (or more generally, Nash equilibrium) includes
 135 a dispersive phenotype, supports at least one sink patch and supports no source patches.
 136 We are able to prove this result only under the restriction that the dispersal matrix S is
 137 *diagonally similar to a symmetric matrix*: there exists an invertible diagonal matrix D such
 138 that DSD^{-1} is a symmetric matrix. This allows for a diversity of movement patterns in-
 139 cluding diffusive movement (i.e. symmetric S) and any form of local movement along a
 140 one-dimensional gradient (i.e. tridiagonal S). A proof is given in Appendix A. It is an open
 141 problem whether this result extends to all irreducible stochastic matrices S .

142 **Theorem 2.** *If $p = 2$, S is diagonally similar to a symmetric matrix, $\mathbf{F}(2, \hat{\mathbf{x}}(2)) \neq \mathbf{F}(1, \hat{\mathbf{x}}(1))$*
 143 *(i.e. there is temporal heterogeneity), and $\mathbf{F}(t, \hat{\mathbf{x}}(t))$ is non-scalar for some t (i.e. there is*
 144 *some spatial heterogeneity), then*

- 145 (i) *If $\max_i d_i = 0$, then $\mathcal{I}(\mathbf{d}; \tilde{d}) > 1$ for all $0 < \tilde{d} \leq 1$.*
 146 (ii) *If \mathbf{d} is a (possibly mixed) Nash equilibrium, then $\max_i d_i > 0$, the set $\mathcal{Sinks} \subset$*
 147 *$\{1, \dots, n\}$ of sink patches is non-empty, and the remaining patches $\{1, \dots, n\} \setminus \mathcal{Sinks}$*
 148 *are balanced.*

149 4. APPLICATIONS

150 To illustrate the utility of our results, we present two applications. The first application
 151 considers populations with compensating density dependence in a periodically forced envi-
 152 ronment. We use Theorem 2 and its proof to determine under what conditions there is an

153 ESC of sedentary and dispersive phenotypes. The second application considers populations
 154 with sufficiently overcompensatory density dependence to create oscillatory dynamics. We
 155 use the proof of Theorem 2 to illustrate how the evolution of higher dispersal rates can
 156 synchronize initially asynchronous population dynamics.

157 **4.1. Evolution of dispersal dimorphisms in periodic environments.** We consider
 158 competing dispersive phenotypes whose within patch dynamics are given by a periodically
 159 forced Beverton-Holt model. For simplicity, we assume that only the intrinsic fitness λ_t^j of
 160 an individual living in patch j varies in time and space:

$$(4.4) \quad f^j(t, \|\mathbf{x}^j\|) = \frac{\lambda_t^j}{1 + a\|\mathbf{x}^j\|}$$

161 where a measures the intensity of competition within a patch. Also for simplicity, we assume
 162 that $S_{kj} = 1/n$ for all j, k . In other words, dispersing individuals are uniformly distributed
 163 across the landscape.

164 When there is only one dispersive phenotype (i.e. $m = 1$), equation (2.1) is a sublinear
 165 monotone map (see, e.g., [25] for definitions). Consequently, [25, Thm. 6.1] implies that the
 166 fate of the population depends on the linearization of the system at the extinction state.
 167 The dominant eigenvalue associated with this linearization is given by

$$\lambda = \varrho \left(\prod_{t=1}^p \mathbf{S}(d_1) \mathbf{F}(t, 0) \right)^{1/p}.$$

168 If $\lambda \leq 1$, then population goes deterministically toward extinction i.e. $\mathbf{x}(t)$ converges to 0 for
 169 all $\mathbf{x}(0) \geq 0$. Alternatively, if $\lambda > 1$, then the populations increases when rare and ultimately
 170 converges to a periodic orbit. More precisely, there exists a periodic orbit, $\{\hat{\mathbf{x}}(1), \dots, \hat{\mathbf{x}}(p)\}$
 171 with $\hat{\mathbf{x}}(t) \gg 0$ for all t , such that $\mathbf{x}(t)$ converges to this periodic orbit whenever $\mathbf{x}(0) \gg 0$.
 172 A sufficient condition ensuring $\lambda > 1$ is

$$(4.5) \quad \left(\prod_{t=1}^p \lambda_t^j \right)^{1/p} > 1 \text{ for all } j.$$

173 In other words, all the patches can support a population in the absence of immigration.
 174 While this condition is stronger than what is necessary, for simplicity, we assume that (4.5)
 175 holds for the remainder of this section.

176 For period two environments where the intrinsic fitness vary in space and time, Theorem 2
 177 implies that a sedentary strategy (i.e. $d_1 = 0$) is not a Nash equilibrium as it can be invaded

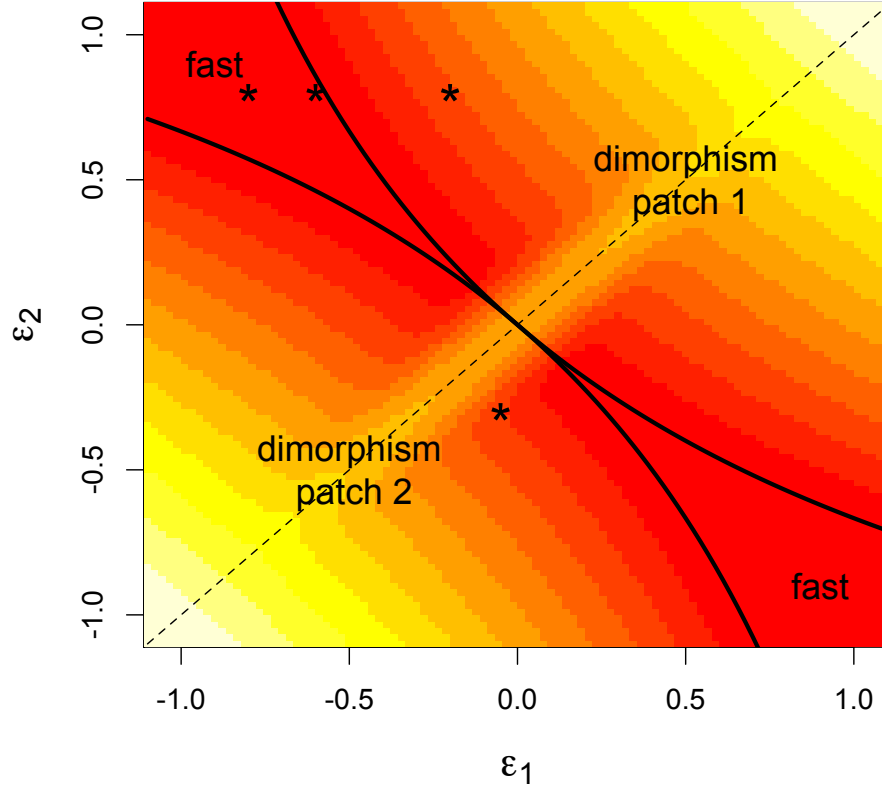


FIGURE 1. Nash equilibria for a Beverton-Holt two patch model with $\lambda_t^1 = 2 + \epsilon_t$ and $\lambda_t^2 = 2 - \epsilon_t$. The strategy $d_1 = 1$ is a local ESS in the regions denoted “fast”. The mixed strategy $\mathbf{d} = (1, 0)$ is an ESC in the regions denoted “dimorphism”. For these regions, the sedentary population only resides in the indicated patch. Shading corresponds to the average abundance of the sedentary strategy with lighter colors corresponding to higher abundance. At the dashed line, all (coalitions of) strategies are a (mixed) Nash equilibrium. *s refer to parameter values for which pairwise invasibility plots are shown in Fig. 2

178 by more dispersive phenotypes. In contrast, for a fully dispersive phenotype (i.e. $d_1 = 1$),
 179 there is a periodic point $\hat{\mathbf{x}}(t)$ given by

$$\hat{x}_1^j(t) = \frac{\bar{\lambda}_2 \bar{\lambda}_1 - 1}{a(1 + \bar{\lambda}_t)}$$

180 where $\bar{\lambda}_t = \frac{1}{n} \sum_{j=1}^n \lambda_t^j$ is the spatial average of the intrinsic fitnesses. Along this periodic
 181 orbit, a computation reveals that the within-patch fitnesses satisfy

$$\prod_{t=1}^2 f^j(t, \|\hat{\mathbf{x}}^j(t)\|) = \prod_{t=1}^2 \frac{\lambda_t^j}{\bar{\lambda}_t}.$$

182 Thus, Theorem 2 implies that a necessary condition for $d_1 = 1$ to be a Nash equilibrium is

$$(4.6) \quad \prod_{t=1}^2 \lambda_t^j \leq \prod_{t=1}^2 \bar{\lambda}_t \text{ for all } j$$

183 with a strict inequality for at least one j . This condition for a Nash equilibrium requires
 184 that the geometric mean of the fitness within each patch is no greater than geometric mean
 185 of the spatially averaged fitness.

186 To illustrate the utility of (4.6), consider an environment where the fitness in each patch
 187 fluctuates between a low value λ_{bad} in “bad” years and a higher value λ_{good} in “good” years
 188 i.e. $\lambda_t^j \in \{\lambda_{good}, \lambda_{bad}\}$, $\lambda_{bad} < \lambda_{good}$, and $\lambda_t^j \neq \lambda_{t+1}^j$. To ensure that all dispersal phenotypes
 189 can persist, we assume that the geometric mean $\sqrt{\lambda_{good}\lambda_{bad}}$ is greater than one. Provided
 190 that there is some spatial asynchrony (i.e. $\lambda_t^j \neq \lambda_t^k$ for some k, j), the necessary condition
 191 (4.6) for a Nash equilibrium of highly dispersive phenotypes simplifies to

$$\sqrt{\lambda_{good}\lambda_{bad}} \leq \frac{1}{2}(\lambda_{good} + \lambda_{bad}).$$

192 This inequality holds strictly as the geometric mean is less than the arithmetic mean. Fur-
 193 thermore, a computation reveals that the geometric mean of fitness within patch j satisfies

$$\sqrt{\prod_{t=1}^2 f^j(t, \|\hat{\mathbf{x}}^j(t)\|)} = \sqrt{\frac{\lambda_{good}\lambda_{bad}}{\frac{1}{4}(\lambda_{good} + \lambda_{bad})^2}} < 1$$

194 for all patches j . Hence, Theorem 3 in Appendix A implies that $\mathcal{I}(1; \tilde{d}) < 1$ for all $\tilde{d} \in [0, 1)$.
 195 Therefore, for this environment, a highly dispersive phenotype ($d_1 = 1$) always is an ESS
 196 and all patches are sinks for populations playing this ESS.

197 When the necessary condition (4.6) for a highly dispersive phenotype to be a Nash equilib-
 198 rium is not met, sedentary dispersers can invade the patches whose average fitness $\sqrt{\prod_{t=1}^2 \lambda_t^j}$
 199 exceeds the spatially averaged fitness $\sqrt{\prod_{t=1}^2 \bar{\lambda}_t}$. To understand the implications of this in-
 200 vasion, we consider a two patch environment where environmental fluctuations are spatially
 201 asynchronous. More precisely, we assume that spatial average of fitness does not vary in
 202 time (i.e. $\bar{\lambda}_t = \bar{\lambda}$) and the temporal fluctuations $\epsilon_t \in (-\bar{\lambda}, \bar{\lambda})$ around this spatial average are

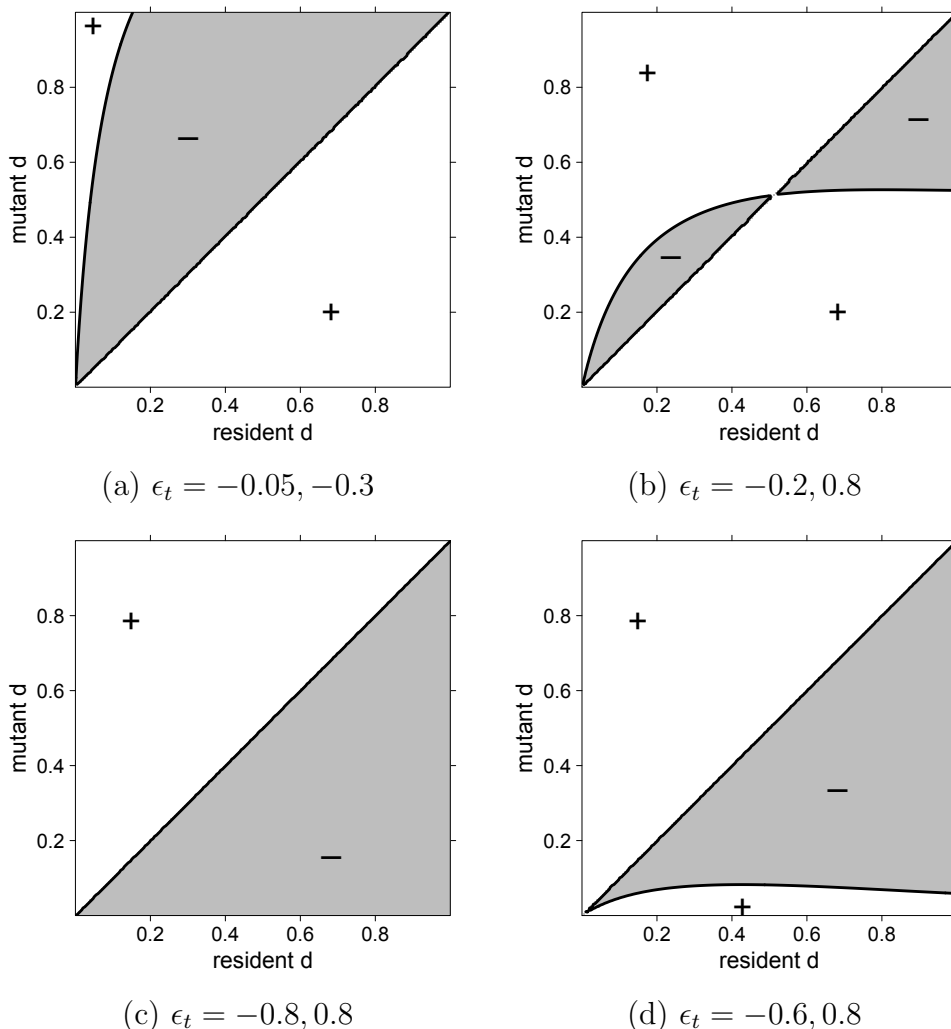


FIGURE 2. Pairwise invasibility plots (PIPs) for a two patch Beverton-Holt model with $\lambda_t^1 = 2 + \epsilon_t$ and $\lambda_t^2 = 2 - \epsilon_t$. The horizontal and vertical axes correspond to resident d_1 and mutant \tilde{d} dispersal rates, respectively. The dark lines, shaded regions, and unshaded regions correspond to where $\mathcal{I}(d_1, \tilde{d}) = 1$, $\mathcal{I}(d_1, \tilde{d}) < 1$, and $\mathcal{I}(d_1, \tilde{d}) > 1$, respectively. In (a) and (b), $d_1 = 0$ is an evolutionary branching point. In (b), $d_1 \approx 0.5$ is a convergently unstable singular point. In (c), $d_1 = 1$ is convergently stable and evolutionarily stable. In (d), $d_1 = 1$ is convergently stable and a local ESS, but invasible by sufficiently sedentary phenotypes.

203 asynchronous i.e. $\lambda_t^1 = \bar{\lambda} + \epsilon_t$ and $\lambda_t^2 = \bar{\lambda} - \epsilon_t$ for $t = 1, 2$. The necessary condition (4.6) for
 204 a highly dispersive phenotype to be a Nash equilibrium becomes

$$(4.7) \quad \bar{\lambda}|\epsilon_1 + \epsilon_2| \leq |\epsilon_1\epsilon_2| \text{ and } \epsilon_1\epsilon_2 < 0.$$

205 When (4.7) is not met, extensive numerical simulations suggest that after the successful in-
 206 vasion of the sedentary dispersers, the populations approach a period 2 orbit $\hat{\mathbf{x}}(t)$. Moreover,
 207 these simulations suggest that $\mathbf{d} = (1, 0)$ is an ESC and, consequently, a potential evolution-
 208 ary end point consisting of a dimorphism of sedentary and highly dispersive phenotypes. At
 209 this ESC, one patch is balanced and occupied by both phenotypes, while the other patch is
 210 a sink and only occupied by the dispersive phenotype. (4.7) implies that the ESC occurs
 211 when the temporal correlations of within patch fitness are not too negative (i.e. ϵ_1 is not
 212 too close to $-\epsilon_2$ in Fig. 1). Pairwise invasibility plots (see, e.g., [26] for a discussion of the
 213 interpretation of these plots and the associated terminology) suggest that these ESCs can
 214 be reached by small mutational steps when $d = 0$ is a convergently stable branching point
 215 (Fig. 2a,b). On the other hand, when (4.7) is satisfied, the highly dispersive phenotype
 216 may or may not be an ESS in the strict sense (Fig. 2c,d). Although numerical simulations
 217 confirm that the highly dispersive phenotype resists invasion attempts by nearby phenotypes
 218 (i.e. $\mathcal{I}(1, \tilde{d}) \leq 1$ whenever \tilde{d} is sufficiently close to 1), relatively sedentary phenotypes still
 219 may be able invade (Fig. 2d).

220 **4.2. Evolution of synchronicity.** Biotic interactions can generate oscillatory dynamics
 221 and, thereby, temporal variation in fitness. To illustrate the feedbacks between evolution
 222 of dispersal and biotically generated oscillations, we consider an extension of the coupled
 223 Logistic map introduced by Hastings [27]. In this model, the local dynamics are determined
 224 by the Logistic fitness function $rx(1-x)$. A fraction d of all individuals disperses randomly
 225 to all patches i.e. a fraction d/k of individuals from patch j arrives in all patches. Under
 226 these assumptions, the dynamics of a single dispersive phenotype is given by

$$x_{t+1}^j = (1-d)r x_t^j(1-x_t^j) + \frac{d}{n} \sum_{k=1}^n r x_t^k(1-x_t^k)$$

227 We note that in the case of $n = 2$ patches, Hastings's d corresponds to our $d/2$.

228 When $r > 3$ and there are two patches, Hastings [27] has shown that there is an interval
 229 of dispersal rates between 0 and 1 such that there is an out-of-phase stable period two point
 230 (Figs. 3a,c,d). To apply our results, let $m = 1$, $d_1 = d$ for which there is a stable out-
 231 of-phase periodic point, $\hat{\mathbf{x}}(1), \hat{\mathbf{x}}(2)$ (an explicit formula for this orbit can be found in the
 232 Appendix of [27]), $S_{jk} = 1/2$ for $1 \leq j, k \leq 2$, and $f^j(t, \|\mathbf{x}^j\|) = r(1 - \|\mathbf{x}^j\|)$. Along this
 233 out-of-phase periodic orbit, $\prod_t \mathbf{F}(t, \hat{\mathbf{x}}(t))$ is a scalar matrix. Hence, Theorem. 3 implies that
 234 along this out-of-phase periodic orbit $\mathcal{I}(d_1, \tilde{d}) > 1$ for all $d_1 < \tilde{d} \leq 1$. Hence, there would be

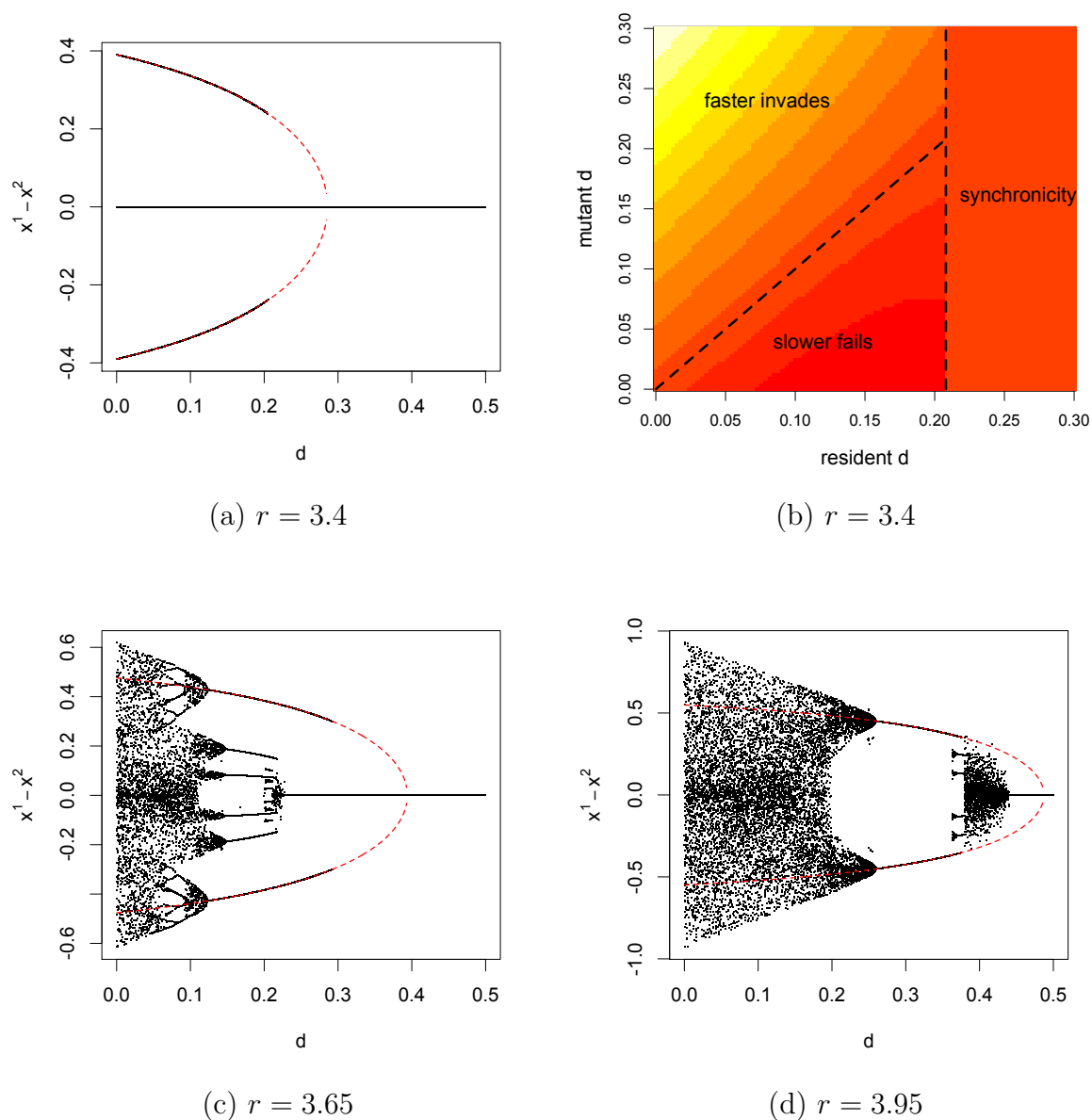


FIGURE 3. Evolution of spatial synchronization in a two-patch Logistic model. In (a), (c), (d), orbital bifurcation diagrams for phase difference $x^1 - x^2$ are shown for for the two-patch Logistic equation. All phase differences along attractors are plotted in black. The red dashed curve corresponds to the out-of-phase, period two orbit which is stable only when it overlaps the black regions. In (b), the contours of $\mathcal{I}(d; \tilde{d})$ are plotted along the out-of-phase periodic point whenever it is stable.

235 selection for higher dispersal rates. For this two patch case, this implication of Theorem 3
 236 also follows from a proposition of Doebeli and Ruxton [10, pg. 1740] in which they performed
 237 a direct calculation of the eigenvalues. For $3 < r \leq 3.7$, numerical simulations suggest that

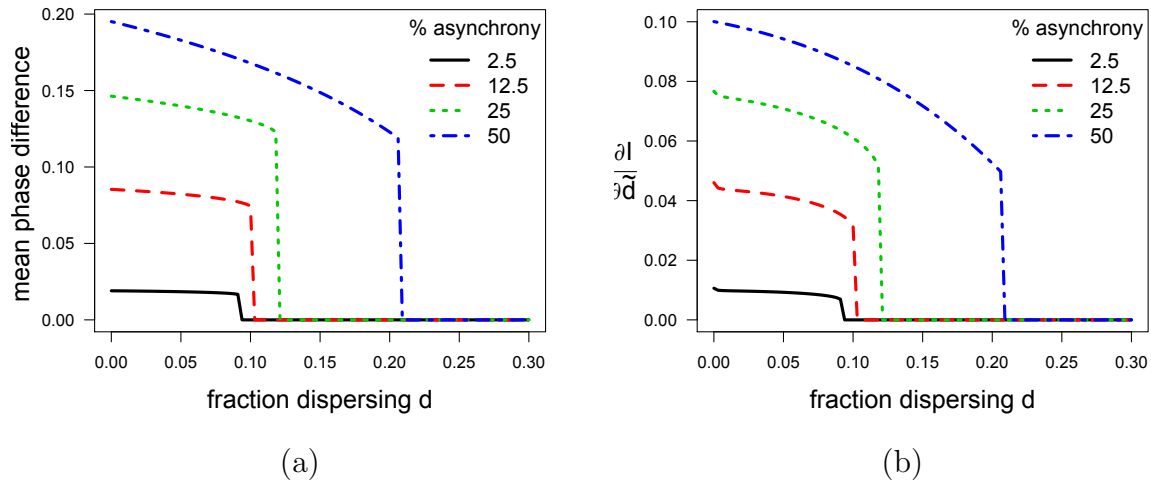


FIGURE 4. Evolution of spatial synchronization for a 40 patch Logistic model. In (a), the mean phase difference in spatial abundance (i.e. $\frac{1}{40^2} \sum_{j \neq k} |x^j - x^k|$) for a single population exhibiting a two-cycle is plotted as function of its dispersal rate. In (b), the strength of selection $\frac{\partial \bar{f}}{\partial d}(d, d)$ for higher dispersal rates is plotted as a function of its dispersal rate. Different lines correspond to different percentages of initial asynchrony for sedentary phenotype e.g. 50% implies that half the patches at $d = 0$ were out of sync with the other set of patches.

238 this selection for higher dispersal rates ultimately results in a dispersal rate that spatially
 239 synchronizes the dynamics (Figs. 3a-c) at which point all dispersal rates are Nash equilibria.
 240 However, at higher r values such as $r = 3.95$ (Fig. 3d), the destabilization of the out-of-phase
 241 period 2 point (at $d_1 \approx 0.38$) results in more complex asynchronous dynamics in which case
 242 our results are not applicable and evolution of dispersal may no longer synchronize the
 243 dynamics.

244 When there are more than two patches and $r > 3$, out-of-phase 2 cycles can take on a
 245 greater diversity of forms. In particular, one can divide the landscape into two sets of patches
 246 such that patches are synchronous within each set and asynchronous across sets. Due to this
 247 potential spatial asymmetry in these out-of-phase cycles, we have not been able to show
 248 the geometric mean of fitness equals one in all patches. However, numerical simulations for
 249 $n = 40$ patches and $3 < r < 3.45$, suggest that this does occur. In which case, Theorem 3
 250 implies that there would selection for higher dispersal rates along these asynchronous cycles.
 251 In fact, numerical simulations for $3 < r < 3.45$ show that there would be selection for
 252 higher dispersal rates until the dynamics are spatially synchronized (Fig. 4). Moreover,

253 these simulations show, quite intuitively, greater initial asynchrony for the dynamics of the
254 sedentary phenotype result in a stronger selection gradient (Fig. 4b) and require the evolution
255 of higher dispersal rates to regionally synchronize the dynamics (Fig. 4a).

256

5. DISCUSSION

257 We analyzed the evolution of dispersal in spatially and temporally variable environments.
258 When there is spatial variation in fitness and within patch fitness varies in time between a
259 lower and higher value, we proved that any evolutionary stable strategy (ESS) or evolution-
260 arily stable coalition (ESC) includes a dispersive phenotype. In particular, our results imply
261 a sedentary population can be always be invaded by more dispersive phenotypes. These
262 results are particularly remarkable in light of earlier analysis showing generically the only
263 ESS for spatially heterogenous environments without temporal heterogeneity is a sedentary
264 phenotype [3, 12, 16, 20]. Hence, our results imply this earlier work on discrete-time models
265 is not generic: arbitrarily small periodic perturbations result in selection for dispersal.

266 Our results extend a result of Parvinen [20] who proved sedentary phenotypes could be
267 invaded by phenotypes that disperse uniformly to all patches in every generation. Moreover,
268 they are consistent with the numerical work of Mathias et al. [13] who found that ESCs
269 always included highly dispersive phenotypes in discrete-time models with random variation
270 in the vital rates. In contrast, our results are only partially consistent with the analysis of
271 reaction-diffusion models by Hutson et al. [15]. Hutson et al. proved that certain forms of
272 spatio-temporal heterogeneities select for the higher dispersal rate. However, if the frequency
273 of spatial oscillations (i.e. spatial variation) is too large or too small, then phenotypes with
274 higher dispersal rates are driven to extinction. A partial explanation for this discrepancy
275 is the continuity of the per-capita growth rates in the reaction-diffusion models results in
276 positive correlations in time which may select for slower dispersal rates.

277 Our analysis and numerical simulations suggest that there are two evolutionary end states
278 for environments where spatial-temporal heterogeneity is generated by abiotic periodic forc-
279 ing: either an ESS consisting of a highly dispersive phenotype or an ESC consisting of a
280 highly dispersive phenotype and a sedentary phenotype. This is partially consistent with the
281 numerical work of Mathias et al. [13] who always found ESCs of high and low dispersal phe-
282 notypes. Mathias et al. found that these ESC always could be achieved by small mutational
283 steps leading to an intermediate phenotype (a convergent singular strategy) at which coali-
284 tions of faster and slower dispersers could invade and coexist (evolutionary branching). Our

285 numerical and analytic results differ from these conclusions in two ways. First, evolutionary
286 branching occurs at sedentary phenotypes not intermediate phenotypes. Consequently, prior
287 to the branching event, one of the strategies in the ESC is already present. Second, while
288 evolution by small mutational states may culminate in a highly dispersive phenotype, an
289 ESC of highly dispersive and sedentary phenotypes may arise by the invasion of sufficiently
290 slow dispersers i.e. large mutational steps are required to realize the ESC.

291 When spatial and temporal heterogeneity is created purely by biotic interactions and
292 initial conditions (e.g. the coupled Logistic map), we have shown there can be selection
293 for higher dispersal rates that ultimately may synchronize the population dynamics across
294 space. Following this synchronization event, dispersal would become selectively neutral. Our
295 analytic results extend Doebeli and Ruxton's [10] two-patch analysis to multiple patches. In
296 a multispecies context, Dercole et al. [21] found a related result. Numerical simulations of
297 tritrophic communities with chaotic dynamics showed that evolution of dispersal often drove
298 these spatial networks to weak forms of synchronization.

299 Our analysis states that an ESS or a ESC for dispersal result in some patches being sinks
300 (i.e. geometric mean of fitness less than one) and the remaining patches being balanced
301 (i.e. geometric mean of fitness equal to one). In the case of ESCs of highly dispersive and
302 sedentary phenotypes, the sedentary phenotypes only reside in the balanced patches. In the
303 case of ESS of highly dispersive phenotypes, all patches may be sinks despite the population
304 persisting. In contrast, evolutionarily stable strategies for conditional dispersal in purely spa-
305 tially heterogenous environments result in all occupied patches being balanced [16, 18] and,
306 thereby, exhibiting an ideal and free distribution [1]. By appropriately modifying empirical
307 methods for distinguishing between source-sink dynamics and balanced-dispersal [11, 29], one
308 might be able to find empirical support for these alternative, evolutionarily stable, spatial-
309 temporal patterns of fitness.

310 Despite extensive progress, there are many mathematical challenges to overcome if we want
311 to have a better analytical understanding of the evolution of dispersal. Two challenges, of
312 particular interest here, are going beyond the assumption period 2 environments, and ac-
313 counting for various forms of costs for dispersal. While period 2 environments can be viewed
314 as a crude cartoon of seasonal environments, most environmental fluctuations exhibit multi-
315 ple modes in their Fourier decomposition and have a significant stochastic component [30].
316 Despite some progress [31, 32], a detailed analytic understanding of the interactive effects
317 of this environmental stochasticity and dispersal on regional fitness remains largely elusive.

318 Alternatively, the ability to disperse or the act of dispersing often is accompanied by costs
 319 to the individual. Dispersing individuals may die before reaching their destination. Alter-
 320 natively, there may trade-offs between dispersal ability and competitive abilities [33, 34]. If
 321 these costs or tradeoffs are sufficiently strong, they can substantially alter the predictions
 322 presented here. For example, Parvinen [20] has shown, quite intuitively, that if costs to dis-
 323 persal are sufficiently strong, there is always selection against dispersal. However, we need
 324 the development of new mathematical methods to unravel the implications of intermediate
 325 costs on the evolution of dispersal in environments with spatio-temporal variation.

326 APPENDIX A. PROOF OF THEOREM 2

327 The proof of Theorem 2 depends on the following key result which is proven in Appendix
 328 B. We do not impose the assumption that S is irreducible in this result.

Theorem 3. *Let $D = \text{diag}(d_1, \dots, d_n)$ with $d_1, \dots, d_n \in (0, \infty)$, and let S be an $n \times n$ column stochastic matrix such that RSR^{-1} is symmetric for some diagonal matrix R . For $t \in [0, 1]$, denote by $\rho(F(t))$ the Perron (largest) eigenvalue of*

$$F(t) = D[(1-t)I_n + tS]D^{-1}[(1-t)I_n + tS].$$

329 *Then $\rho(F(t))$ is either an increasing function on $[0, 1]$ or a constant function on $[0, 1]$. The
 330 latter case happens if and only if D and S commute, equivalently, there is a permutation
 331 matrix P such that $PSP^T = S_1 \oplus S_2 \oplus \dots \oplus S_k$ and $PDP^T = d_1 I_{n_1} \oplus d_2 I_{n_2} \oplus \dots \oplus d_k I_{n_k}$,
 332 where $S_j \in M_{n_j}$ for $j = 1, \dots, k$, and $n_1 + \dots + n_k = n$.*

333 **Remark.** The above result covers the case of symmetric S . It also covers the case when
 334 S is an irreducible tridiagonal column stochastic matrix; one can use a simple continuity
 335 argument to extend the result to reducible tridiagonal column stochastic matrices.

336 To prove the first assertion of Theorem 2, assume that $\max_i d_i = 0$. Assumption **A2**
 337 implies that $\mathbf{F}(2, \hat{\mathbf{x}}(2))\mathbf{F}(1, \hat{\mathbf{x}}(1)) = I$. Theorem 3 implies $\mathcal{I}(\mathbf{d}; \tilde{d}) > 1$ for all $\tilde{d} \in (0, 1]$.

338 To prove the second assertion of Theorem 2, assume that \mathbf{d} is a (possibly mixed) Nash
 339 equilibrium. The first assertion of the Theorem implies that $\max_i d_i > 0$. Next, suppose
 340 to the contrary that there exists j such that $f^j(1, \|\hat{\mathbf{x}}^j(1)\|)f^j(2, \|\hat{\mathbf{x}}^j(2)\|) > 1$ i.e. there is a
 341 source patch. Then

$$\mathcal{I}(\mathbf{d}; 0) = \max_j \sqrt{f^j(1, \|\hat{\mathbf{x}}^j(1)\|)f^j(2, \|\hat{\mathbf{x}}^j(2)\|)} > 1$$

342 and by continuity $\mathcal{I}(\mathbf{d}; \tilde{d}) > 1$ for all $\tilde{d} \geq 0$ sufficiently small. As this contradicts the
 343 assumption that \mathbf{d} is a Nash coalition, it follows that $f^j(1, \|\hat{\mathbf{x}}^j(1)\|)f^j(2, \|\hat{\mathbf{x}}^j(2)\|) \leq 1$ for all
 344 j . Finally, suppose to the contrary that $f^j(1, \|\hat{\mathbf{x}}^j(1)\|)f^j(2, \|\hat{\mathbf{x}}^j(2)\|) = 1$ for all j . Theorem 3
 345 implies that $\mathcal{I}(\mathbf{d}; \max_i d_i) > 1$ which contradicts the fact that $\mathcal{I}(\mathbf{d}; \max_i d_i) = 1$.

346 APPENDIX B. PROOF OF THEOREM 3

347 Denote by $\|A\|$ the operator norm of the matrix A . The proof of Theorem 3 depends on
 348 the following.

349 **Theorem 4.** *Suppose $A \in M_n$ is nonzero and satisfies $\|I+A\| \geq 1$. Then $\|I+tA\| \geq \|I+A\|$
 350 for all $t \geq 1$ and one of the following condition holds.*

351 (a) *The function $t \mapsto \|I + tA\|$ is increasing for $t \geq 1$.*

352 (b) *There is a unitary matrix U such that $U^*AU = 0_k \oplus \tilde{A}$, where $\tilde{A} \in M_{n-k}$ is invertible
 353 and satisfies $\|I_{n-k} + \tilde{A}\| < 1$. Consequently, there is $t^* > 1$ such that $\|I_{n-k} + t^*\tilde{A}\| = 1$ and
 354 the function $t \mapsto \|I + tA\|$ has constant value 1 for $t \in [1, t^*]$ and is increasing for $t > t^*$.*

Proof. Let u be a unit vector such that $\|I + A\| = \|(I + A)u\|$ and $Au = \alpha u + \beta v$, where $\{u, v\}$ is an orthonormal family. By our assumption,

$$\|(I + A)u\| = \|(1 + \alpha)u + \beta v\| = |1 + \alpha|^2 + |\beta|^2 \geq 1,$$

i.e.,

$$2\operatorname{Re}(\alpha) + |\alpha|^2 + |\beta|^2 \geq 0.$$

355 Thus, for $t > 1$,

$$\begin{aligned} \|I + tA\| &\geq \|(I + tA)u\| \\ &= |1 + t\alpha|^2 + |t\beta|^2 \\ &= |1 + \alpha|^2 + |\beta|^2 + 2(t-1)\operatorname{Re}(\alpha) + (t^2-1)[|\alpha|^2 + |\beta|^2] \\ &= \|I + A\| + (t-1)[2\operatorname{Re}(\alpha) + |\alpha|^2 + |\beta|^2] + t(t-1)[|\alpha|^2 + |\beta|^2] \\ &\geq \|I + A\|. \end{aligned}$$

356 (a) Suppose there is unit vector u in the above calculation satisfying $Au \neq 0$, i.e., $(\alpha, \beta) \neq$
 357 $(0, 0)$. Then the last inequality in the calculation is a strict inequality. Thus, $\|I + tA\| >$
 358 $\|I + A\|$.

Now, for any $t_0 > 1$, we have $\|I + t_0A\| > \|I + A\| \geq 1$. If u_0 is a unit vector satisfying $\|(I + t_0A)u_0\| = \|I + t_0A\|$, then $t_0Au_0 \neq 0$; otherwise, $\|I + t_0A\| = 1$. Consequently, if we replace A by t_0A in the above proof, we have

$$\|I + t(t_0A)\| > \|I + t_0A\|$$

359 for any $t \geq 1$. Thus the function $t \mapsto \|I + tA\|$ is increasing for $t > 1$.

(b) Suppose $Au = 0$ for every unit vector u satisfying $\|(I + A)u\| = \|I + A\|$. In particular, we have

$$\|I + A\| = \|(I + A)u\| = \|u\| = 1.$$

Let U be unitary such that U^*AU is lower triangular form with the first k diagonal entries equal to zero, and the last $n - k$ diagonal entries nonzero. Since

$$\|I + A\| = \|I + U^*AU\| = 1,$$

we see that

$$e_j^*(I + U^*AU)^*(I + U^*AU)e_j = \|(I + U^*AU)e_j\|^2 \leq 1$$

360 for $j = 1, \dots, k$. (Here $\{e_1, \dots, e_n\}$ is the standard basis for \mathbb{C}^n .) As a result, we see that
 361 $U^*AU = 0_k \oplus \tilde{A}$, where $\tilde{A} \in M_{n-k}$ is invertible.

362 Since $Au = 0$ for every unit vector u satisfying $\|(I + A)u\| = \|I + A\| = 1$, we conclude
 363 that $\|(I_{n-k} + \tilde{A})v\| < 1$ for any unit vector $v \in \mathbb{C}^{n-k}$. Thus, $\|I_{n-k} + \tilde{A}\| < 1$.

364 Note that $A \neq 0$ implies \tilde{A} is non-trivial, i.e., $k \neq n$. For sufficiently large t , we have
 365 $\|I_{n-k} + t\tilde{A}\| \geq 1$. Let t^* be the smallest real number in $(1, \infty)$ such that $\|I_{n-k} + t^*\tilde{A}\| = 1$.
 366 Since \tilde{A} is invertible, case (a) must hold and the function $t \mapsto \|I_{n-k} + t\tilde{A}\|$ is increasing for
 367 $t \geq t^*$. Hence for $t \geq t^*$, we have $\|I + tA\| = \|I_{n-k} + \tilde{A}\|$ and the function $t \mapsto \|I + tA\|$ is
 368 increasing. ■

369 *Proof of Theorem 3.* Note that $F(t) = D[(1 - t)I_n + tS]D^{-1}[(1 - t)I_n + tS]$ and

$$\begin{aligned} \tilde{F}(t) &= RF(t)R^{-1} \\ &= RDR^{-1}[(1 - t)I_n + tRSR^{-1}]RD^{-1}R^{-1}[(1 - t)I_n + tRSR^{-1}] \\ &= D[(1 - t)I_n + tRSR^{-1}]D^{-1}[(1 - t)I_n + tRSR^{-1}] \end{aligned}$$

have the same eigenvalues and hence the same spectral radius. Here, we use the fact that $RDR^{-1} = D$ as R is a diagonal matrix. So, $\tilde{S} = RSR^{-1}$ is symmetric with largest eigenvalue equal to 1, and all other eigenvalues lying in $[-1, 1]$. Moreover, if

$$B(t) = D^{1/2}[(1 - t)I_n + t\tilde{S}]D^{-1/2},$$

370 then $D^{-1/2}F(t)D^{1/2} = B(t)B(t)^T$ so that $\varrho(F(t)) = \varrho(D^{-1/2}F(t)D^{1/2}) = \|B(t)\|^2$.

Suppose $0 \leq t_0 < t_0 + t \leq 1$. Let $A_0 = t_0 D^{1/2}(\tilde{S} - I_n)D^{-1/2}$. Then

$$\|I + A_0\| = \|B(t_0)\| \geq \varrho(B(t_0)) = 1.$$

371 By Theorem 4,

$$(B.8) \quad \|B(t_0 + t)\| = \|I + (1 + t/t_0)A_0\| \geq \|I + A_0\| = \|B(t_0)\|.$$

372 Thus, $\varrho(F(t)) = \|B(t)\|^2$ is non-decreasing on $[0, 1]$. Moreover, by Theorem 4 the inequality

373 in (B.8) is an equality if and only if A_0 is unitarily similar to $0_k \oplus \tilde{A}_0$ where \tilde{A}_0 is invertible.

374 Thus,

375 (1) the null space of A_0 has dimension k , and

376 (2) $A_0 v = 0$ if and only if $v^T A_0 = 0$.

377 From (1), we see that the eigenspace of the Perron root of the matrix $D^{1/2}\tilde{S}D^{-1/2}$ has

378 dimension k . So, the matrix is permutationally similar to a $(k+1) \times (k+1)$ upper triangular

379 block matrix so that each of the first k diagonal block is square irreducible and has eigenvalue

380 1, and the last block has eigenvalue less than 1. Since \tilde{S} is symmetric and D is diagonal, there

381 is a permutation matrix P such that $P\tilde{S}P^T = \tilde{S}_1 \oplus \cdots \oplus \tilde{S}_{k+1}$ and $PDP^{-1} = D_1 \oplus \cdots \oplus D_{k+1}$

382 with $\tilde{S}_j, D_j \in M_{n_j}$ and $n_1 + \cdots + n_{k+1} = n$. But then $D_{k+1}^{1/2}\tilde{S}_{k+1}D_{k+1}^{-1/2}$ cannot have spectral

383 radius less than 1. So, S_{k+1} must be vacuous.

384 Next, we show that each D_j is a scalar matrix. To this end, note that we can construct a

385 null vector of PA_0P^T by extending a Perron vector $u_1 \in \mathbb{R}^{n_1}$ of \tilde{S}_1 to a vector v_1 in \mathbb{R}^n by

386 adding $n - n_1$ zeros. Then $PA_0P^T v_1 = 0$. By (2), we see that $v_1^T PA_0P^T = 0$. It follows that

387 $D_1^{1/2}\tilde{S}_1D_1^{-1/2}u_1 = u_1$ and $u_1^T D_1^{1/2}\tilde{S}_1D_1^{-1/2} = u_1^T$. Equivalently, $\tilde{S}_1D_1^{-1/2}u_1 = D_1^{-1/2}u_1$ and

388 $u_1^T D_1^{1/2}\tilde{S}_1 = u_1^T D_1^{1/2}$. Since \tilde{S}_1 is symmetric, nonnegative, and irreducible, the eigenspace of

389 the Perron eigenvalue is one dimensional and there is a positive vector w such that $\tilde{S}_1 w = w$

390 and $w^T \tilde{S}_1 = w^T$. Hence $D_1^{-1/2}u_1$ is a multiple of w and $u_1^T D_1^{1/2}$ is a multiple of w^T . Hence

391 D_1 is a scalar matrix. Similarly, one can prove that D_2, \dots, D_k are scalar matrices. Since

392 $P\tilde{S}P^T = \tilde{S}_1 \oplus \cdots \oplus \tilde{S}_k$, we have $PSP^T = S_1 \oplus \cdots \oplus S_k$.

393 Conversely, if S and D commute, then $F(t) = (tI + (1-t)S)(tI + (1-t)S)$ is column

394 stochastic for all $t \in [0, 1]$. So, $\varrho(F(t)) = 1$ for all $t \in [0, 1]$. ■

395 **Remark** Note that the conclusion of Theorem 3 fails if S is not diagonally similar to a
 396 symmetric matrix. For example, if $S = \begin{pmatrix} 0 & 1 & 0 \\ 0 & 0 & 1 \\ 1 & 0 & 0 \end{pmatrix} \oplus I_{n-3}$, and $D = \text{diag}(3, 2, 1) \oplus I_{n-3}$,
 397 then $\varrho(F(0)) = \varrho(F(1)) = 1$, but $\varrho(F(1/2)) > 1$. One may perturb S slightly, say, replacing
 398 it by $(1 - \varepsilon)S + \varepsilon J$ for a small $\varepsilon > 0$ so that $\varrho(F(t))$ is not monotone, where J is the matrix
 399 with all entries equal to $1/n$.

400 **Acknowledgements.** We thank two anonymous reviewers and Fabio Dercole for their
 401 extensive and helpful comments. The research of the first author was partially supported by
 402 U.S. National Science Foundation Grants DMS-0517987 and EF-0928987. The research of
 403 the second author was partially supported by the U.S. National Science Foundation and the
 404 William and Mary Plumeri Award. He is an honorary professor of the University of Hong
 405 Kong and an honorary professor of the Taiyuan University of Technology.

406 REFERENCES

- 407 [1] S. D. Fretwell and H. L. Jr. Lucas. On territorial behavior and other factors influencing
 408 habitat distribution in birds. *Acta Biotheoretica*, 19:16–36, 1970.
- 409 [2] W. D. Hamilton and R. May. Dispersal in stable habitats. *Nature*, 269:578–581, 1977.
- 410 [3] A. Hastings. Can spatial variation alone lead to selection for dispersal? *Theoretical*
 411 *Population Biology*, 24:244–251, 1983.
- 412 [4] S. A. Levin, D. Cohen, and A. Hastings. Dispersal strategies in patchy environments.
 413 *Theoretical Population Biology*, 26(2):165 – 191, 1984.
- 414 [5] R. D. Holt. Patch dynamics in two-patch environments: Some anomalous consequences
 415 of an optimal habitat distribtuion. *Theor. Pop. Biol.*, 28:181–208, 1985.
- 416 [6] H. R. Pulliam. Sources, sinks, and population regulation. *Amer. Nat.*, 132:652–661,
 417 1988.
- 418 [7] D. Cohen and S. A. Levin. Dispersal in patchy environments: the effects of temproal
 419 and spatial structure. *Theor. Pop. Bio.*, 39:63–99, 1991.
- 420 [8] M.A. McPeck and R. D. Holt. The evolution of dispersal in spatially and temporally
 421 varying environments. *American Naturalist*, 6:1010–1027, 1992.
- 422 [9] R. D. Holt. Demographic constraints in evolution: Towards unifying the evolutionary
 423 theories of senescence and niche conservatism. *Evolutionary Ecology*, 10:1573–8477,
 424 1996.

- 425 [10] M. Doebeli and G. D. Ruxton. Evolution of dispersal rates in metapopulation models:
426 Branching and cyclic dynamics in phenotype space. *Evolution*, 51(6):1730–1741, 1997.
- 427 [11] J. E. Diffendorfer. Testing models of source-sink dynamics and balanced dispersal.
428 *Oikos*, 81(3):417–433, 1998.
- 429 [12] J. Dockery, V. Hutson, K. Mischaikow, and M. Pernarowski. The evolution of slow
430 dispersal rates: a reaction diffusion model. *J. Math. Biol.*, 37:61–83, 1998.
- 431 [13] A. Mathias, E. Kisdi, and I. Olivieri. Divergent evolution of dispersal in a heterogeneous
432 landscape. *Evolution*, 55(2):246–259, 2001.
- 433 [14] N. A. Friedenberg. Experimental evolution of dispersal in spatiotemporally variable
434 microcosms. *Ecology Letter*, 6:953–959, 2003.
- 435 [15] V. Hutson, K. Mischaikow, and P. Poláčik. The evolution of dispersal rates in a heteroge-
436 neous time-periodic environment. *J. Math. Biol.*, 43(6):501–533, 2001. ISSN 0303-6812.
- 437 [16] S. Kirkland, C.K. Li, and S. J. Schreiber. On the evolution of dispersal in patchy
438 landscapes. *SIAM Journal on Applied Mathematics*, 66(4):1366–1382, 2006.
- 439 [17] R. S. Cantrell, C. Cosner, and Y. Lou. Movement toward better environments and the
440 evolution of rapid diffusion. *Math. Biosci.*, 204(2):199–214, 2006.
- 441 [18] R.S. Cantrell, C. Cosner, D. L. Deangelis, and V. Padron. The ideal free distribution
442 as an evolutionarily stable strategy. *J. Biol. Dyn.*, 1:249–271, 2007.
- 443 [19] S. J. Schreiber and E. Saltzman. Evolution of predator and prey movement into sink
444 habitats. *American Naturalist*, 174:68–81, 2009.
- 445 [20] K. Parvinen. Evolution of migration in a metapopulation. *Bulletin of Mathematical*
446 *Biology*, 61(3):531–550, 1999.
- 447 [21] F. Dercole, D. Loiacono, and S. Rinaldi. Synchronization in ecological networks: A
448 byproduct of darwinian evolution? *International Journal of Bifurcation and Chaos*, 17
449 (7):2435–2446, 2007.
- 450 [22] A. Katok and B. Hasselblatt. *Modern Theory of Dynamical Systems*. Cambridge Uni-
451 versity Press, 1995.
- 452 [23] S. A. H. Geritz, M. Gyllenberg, F. J. A. Jacobs, and K. Parvinen. Invasion dynamics
453 and attractor inheritance. *J. Math. Biol.*, 44(6):548–560, 2002.
- 454 [24] R. Cressman. *Evolutionary Dynamics and Extensive Form Games*. M.I.T. Press, 2003.
- 455 [25] M. W. Hirsch and H. L. Smith. Monotone maps: a review. *Journal of Difference*
456 *Equations and Applications*, 11:379–398, 2005.

- 457 [26] S.A.H. Geritz, J.A.J. Metz, E. Kisdi, and G. Meszena. Dynamics of adaptation and
458 evolutionary branching. *Physical Review Letters*, 78:2024–2027, 1997.
- 459 [27] A. Hastings. Complex interactions between dispersal and dynamics: Lessons from cou-
460 pled Logistic equations. *Ecology*, 74:1362–1372, 1993.
- 461 [28] A. Hastings and T. Powell. Choas in a three species food chain. *Ecology*, 72:896–903,
462 1991.
- 463 [29] C.P. Doncaster, J. Clobert, B. Doligez, E. Danchin, and L. Gustafsson. Balanced disper-
464 sal between spatially varying local populations: an alternative to the source-sink model.
465 *The American Naturalist*, 150(4):425–445, 1997.
- 466 [30] D. A. Vasseur and P. Yodzis. The color of environmental noise. *Ecology*, 85:1146–1152,
467 2004.
- 468 [31] S. J. Schreiber. Interactive effects of temporal correlations, spatial heterogeneity, and
469 dispersal on population persistence. *Proceedings of the Royal Society: Biological Sci-*
470 *ences*, In press.
- 471 [32] P. Wiener and S. Tuljapurkar. Migration in variable environments: Exploring life-
472 history evolution using structured population models. *Journal of Theoretical Biology*,
473 166:75–90, 1994.
- 474 [33] R. Levins and D. Culver. Regional coexistence of species and competition between
475 rare species. *Proceedings of the National Academy of Sciences of the United States of*
476 *America*, 68(6):1246, 1971.
- 477 [34] D.W. Yu and H.B. Wilson. The competition-colonization trade-off is dead; long live the
478 competition-colonization trade-off. *Am Nat*, 158:49–63, 2001.

479 DEPARTMENT OF EVOLUTION AND ECOLOGY AND CENTER FOR POPULATION BIOLOGY, UNIVERSITY
480 OF CALIFORNIA, DAVIS, CA 95616
481 *E-mail address:* `sschreiber@ucdavis.edu`

482 DEPARTMENT OF MATHEMATICS, COLLEGE OF WILLIAM AND MARY, WILLIAMSBURG, VA
483 *E-mail address:* `ckli@math.wm.edu`